With regard to other candidates that control the migration of NCCs, previous studies have demonstrated that Eph-ephrin and Semaphorin/Neuropilin signaling influences migration of craniofacial NCCs in the mouse as well as in *Xenopus*, chick and zebrafish (Smith *et al.* 1997; Osborne *et al.* 2005; Yu & Moens 2005). Moreover, in human, mutations of *Semaphorin 3E* and *ephrin B1* were found in patients with congenital anomalies associated with neural crest derived tissues (Lalani *et al.* 2004; Twigg *et al.* 2004).

Thus, these genes could be involved in ocular morphogenesis, especially in the NCDC-containing anterior and posterior eye regions. Future studies focusing on molecular and cellular mechanisms of distribution and differentiation of NCCs in the ocular region would provide a clearer answer to the pathogenesis of various ocular malformations in human.

Experimental procedures

Animals

Transgenic mice expressing Cre enzyme driven by myelin protein zero (P0) promoter were crossed with another transgenic lines *CAG-CAT-Z* (Yamauchi *et al.* 1999), or *CAG-CAT-EGFP* (Kawamoto *et al.* 2000). In each double transgenic mouse, NCDCs could be identified by the expression of lacZ or GFP after the P0-Cre mediated DNA recombination. These double transgenic lines were crossed with *Pax6*-heterozygous mice ($Pax6^{Sey/-}$) (Hill *et al.* 1991), kindly provided by Dr van Heyningen. To eliminate pigmentation in the iris tissue of the double transgenic lines, these mice originally of C57/B6J background (black color) were crossed with CD-1 background (albino color) (Japan Charles River, Tokyo, Japan) for 5-6 generations. The mid-day of identifying a vaginal plug was considered as embryonic day (E) 0.5. Genomic DNA was prepared from the yolk sac of embryos or tails of pups. To examine the genotypes, polymerase chain reaction (PCR) analyses for *P0-Cre*, *CAG-CAT-Z* and *CAG-CAT-EGFP* were performed as previously described (Yamauchi *et al.* 1999; Kawamoto *et al.* 2000), in which the enzymatic digestion of specific PCR products was carried out for $Pax6^{Sey/-}$ mice (Grindley *et al.* 1995). All experimental procedures described in the present study were approved by the Ethics Committee for Animal Experiment of Tohoku University Graduate School of Medicine, and animals were treated according to the National Institute of Health guidance for the care and use of laboratory animals.

Detection of β-galactosidase (LacZ) activity in embryos

Embryos were fixed for 45 min at 4 °C with solution containing 1% formaldehyde, 0.2% glutaraldehyde, and 0.02% Norident P-40 in phosphate buffered saline (PBS) as previously described (Yamauchi *et al.* 1999). To detect LacZ activity, embryos were incubated for 30–60 min at 37 °C in a staining solution containing 3 mM potassium ferricyanide, 3 mM potassium ferrocyanide, 1 mM $MgCl_2$, 0.1% TritonX-100 and 2% X-gal in PBS (Suemori *et al.* 1990). Samples were then rinsed 3 times in PBS with 2 mM ethylenediaminetetracetic acid (EDTA) to stop the reaction. Whole-mount staining samples were examined under a stereomicroscope (LEICA CLS-150XD) equipped with a digital camera system (FINGGAL LINK).

Immunohistochemistry

All procedures were performed as previously described (Osumi *et al.* 1997). Detailed information will be provided on request. The following antibodies were used: anti-GFP (rabbit polyclonal, Chemicon); anti-Pax6 (rabbit polyclonal, Inoue *et al.* 2000); anti-BrdU (mouse monoclonal, Becton Dickinson); anti-α smooth muscle actin (mouse monoclonal, Sigma); and anti-PECAM (mouse monoclonal, Becton Dickinson). Then the sections were incubated with Cy3-conjugated goat-anti-mouse IgG (Jackson) or FITC-conjugated goat anti-rabbit IgG (Jackson), and examined with fluorescent microscope (AXIO PLAN-2, ZEISS) equipped with a cooled CCD camera (Roper). To perform enzymatic detection of antibodies, the sections were incubated with Streptavidin-horseradish peroxidase (HRP) complex (VECTASTAIN ABC kit, Vector Laboratories) after secondary antibody incubation. Diamonobenzidine enhance kit (PIERCE) was used to detect HRP activity.

Whole embryo culture and DiI labeling of cranial neural crest cells

Embryos at E 8.25 (1–4 somite stage) were obtained from CD-1 background female mice that were crossed with *P0-Cre*; *CAG-CAT-GFP* double transgenic male mice. The procedures of whole embryo culture and DiI labeling of NCC were based on the methods previously described (Osumi-Yamashita *et al.* 1994). Similarly, the embryos at E10.0 were labeled with DiI in the temporal or nasal side of the periocular mesenchyme. After 36 h culture, the sections were made parallel to the plane along the migration pathway of the midbrain crest cells, and directly observed in the dried condition to see the DiI.

5-bromodeoxyuridine (BrdU) labeling

To analyze cell proliferation, 10 mg/kg BrdU (Boehringer Mannheim, Germany) was injected intraperitoneally into pregnant mice 45 min prior to extraction of embryos. For detection of BrdU-incorporated cells, sections were treated with 2 M HCl solution at 37 °C for 10 min before incubation with anti-BrdU antibody.

Statistical Analysis

Data are expressed as mean ± SD. The two-sample *t*-test was used to compare the data in different groups. A $P < 0.05$ was considered to denote statistical significance.

Acknowledgements

We thank Drs Veronica van Heyningen and Noriyuki Azuma for many valuable comments on the manuscript. We are also grateful to Mss. Michi Otonari, Hisako Yusa, and Ayumi Ogasawara for maintenance of transgenic mouse lines and technical assistance, and all other members of our laboratories for helpful advises. This work was supported by Grants-in Aid for Scientific Research from the Japanese Ministry of Education, Culture, Sports, Science and Technology (No. 10220209, 16015205) (to N.O.). S.K. was supported by the 21st Century COE Program "Future Medical Engineering Based on Bio-nanotechnology."

References

Arai, Y., Funatsu, N., Numayama-Tsuruta, K., Nomura, T., Nakamura, S. & Osumi, N. (2005) Role of FABP-7, a downstream gene of Pax6, in the maintenance of neuroepithelial cells during early embryonic development of the rat cortex. *J. Neurosci.* **25**, 9752–9761.

Azuma, N., Yamaguchi, Y., Handa, H., *et al.* (2003) Mutation of the PAX6 gene detected in patients with a variety of optic-nerve malformations. *Am. J. Hum. Genet.* **72**, 1565–1570.

Baulmann, D.C., Ohlmann, A., Flugel-Koch, C., Goswami, S., Cvekl, A. & Tamm, E.R. (2002) Pax6 heterozygous eyes show defects in chamber angle differentiation that are associated with a wide spectrum of other anterior eye segment abnormalities. *Mech. Dev.* **118**, 3–17.

Chai, Y., Jiang, X., Ito, Y., *et al.* (2000) Fate of the mammalian cranial neural crest during tooth and mandibular morphogenesis. *Development* **127**, 1671–1679.

Chauhan, B.K., Reed, N.A., Yang, Y., *et al.* (2002) A comparative cDNA analysis reveals a spectrum of genes regulated by Pax6 in mouse lens. *Genes Cells* **7**, 1267–1283.

Collinson, J.M., Chanas, S.A., Hill, R.E. & West, J.D. (2004) Corneal development, limbal stem cell function, and corneal epithelial cell migration in the $Pax6^{-/-}$ mouse. *Invest. Ophthalmol. Vis. Sci.* **45**, 1101–1108.

Creuzet, S., Vincent, C. & Couly, G. (2005) Neural crest derivatives in ocular and periocular structures. *Int. J. Dev. Biol.* **49**, 161–171.

Cvekl, A. & Tamm, E.R. (2004) Anterior eye development and ocular mesenchyme: new insights from mouse models and human diseases. *Bioessays* **26**, 374–386.

Danielian, P.S., Muccino, D., Rowitch, D.H., Michael, S.K. & McMahon, A.P. (1998) Modification of gene activity in mouse embryos in utero by a tamoxifen-inducible form of Cre recombinase. *Curr. Biol.* **8**, 1323–1326.

Davis-Silberman, N., Kalich, T., Oron-Karni, V., *et al.* (2005) Genetic dissection of Pax6 dosage requirements in the developing mouse eye. *Hum. Mol. Genet.* **14**, 2265–2276.

Etchevers, H.C., Vincent, C., Le Douarin, N.M. & Couly, G.F. (2001) The cephalic neural crest provides pericytes and smooth muscle cells to all blood vessels of the face and forebrain. *Development* **128**, 1059–1068.

Fujiwara, M., Uchida, T., Osumi-Yamashita, N. & Eto, K. (1994) Uchida rat (rSey): a new mutant rat with craniofacial abnormalities resembling those of the mouse Sey mutant. *Differentiation* **57**, 31–38.

Glaser, T., Jepeal, L., Edwards, J.G., Young, S.R., Favor, J. & Maas, R.L. (1994) PAX6 gene dosage effect in a family with congenital cataracts, aniridia, anophthalmia and central nervous system defects. *Nat. Genet.* **7**, 463–471.

Grant, W.M. & Walton, D.S. (1974) Progressive changes in the angle in congenital aniridia, with development of glaucoma. *Am. J. Ophthalmol.* **78**, 842–847.

Grindley, J.C., Davidson, D.R. & Hill, R.E. (1995) The role of Pax-6 in eye and nasal development. *Development* **121**, 1433–1442.

Hanson, I.M., Fletcher, J.M., Jordan, T., *et al.* (1994) Mutations at the Pax6 locus are found in heterogeneous anterior segment malformations including Peters' anomaly. *Nat. Genet.* **6**, 168–173.

Hanson, I. & Van Heyningen, V. (1995) Pax6: more than meets the eye. *Trends Genet.* **11**, 268–272.

Hasegawa, S., Sato, T., Akazawa, H., *et al.* (2002) Apoptosis in neural crest cells by functional loss of APC tumor suppressor gene. *Proc. Natl. Acad. Sci. USA* **99**, 297–302.

Hay, E.D., Linsenmayer, T.F., Trelstad, R.L. & von der Mark, K. (1979) Origin and distribution of collagens in the developing avian cornea. *Curr. Top. Eye Res.* **1**, 1–35.

Hill, R.E., Favor, J., Hogan, B.L., *et al.* (1991) Mouse small eye results from mutations in a paired-like homeobox-containing gene. *Nature* **354**, 522–525.

Hogan, B.L., Hirst, E.M., Horsburgh, G. & Hetherington, C.M. (1988) Small eye (Sey): a mouse model for the genetic analysis of craniofacial abnormalities. *Development* **103** (Suppl.), 115–119.

Inoue, T., Nakamura, S. & Osumi, N. (2000) Fate mapping of the mouse prosencephalic neural plate. *Dev. Biol.* **219**, 373–383.

Jiang, X., Rowitch, D.H., Soriano, P., McMahon, A.P. & Sucov, H.M. (2000) Fate of the mammalian cardiac neural crest. *Development* **127**, 1671–1679.

Johnston, M.C., Noden, D.M., Hazelton, R.D., Coulombre, J.L. & Coulombre, A.J. (1979) Origins of avian ocular and periocular tissues. *Exp. Eye Res.* **29**, 27–43.

Kawamoto, S., Niwa, H., Tashiro, F., *et al.* (2000) A novel reporter mouse strain that express enhanced green fluorescent protein upon Cre-mediated recombination. *FEBS Lett.* **470**, 263–268.

Kenyon, K.R. (1975) Mesenchymal dysgenesis in Peters anomaly, sclerocornea and congenital endothelial dystrophy. *Exp. Eye Res.* **21**, 124–142.

Korn, J., Christ, B. & Kurz, H. (2002) Neuroectodermal origin of brain pericytes and vascular smooth muscle cells. *J. Comp. Neurol.* **442**, 78–88.

Lalani, S.R., Safiullah, A.M., Molinari, L.M., Fernbach, S.D., Martin, D.M. & Belmont, J.W. (2004) SEMA3E mutation in a patient with CHARGE syndrome. *J. Medical Genet.* 41, e94.

Le Douarin, N.M. & Kalcheim, C. (1999) *The Neural Crest*, 2nd edn. Cambridge, UK: Cambridge University Press.

Mackman, G., Brightbill, F.S. & Optiz, J.M. (1979) Corneal changes in aniridia. *Am. J. Ophthalmol.* **87**, 497–502.

Matsuo, T., Osumi-Yamashita, N., Noji, S., *et al.* (1993) A mutation in the Pax-6 gene in rat small eye is associated with impaired migration of midbrain crest cells. *Nat. Genet.* **3**, 299–304.

Matt, N., Dupe, V., Garnier, J.M., *et al.* (2005) Retinoic acid-dependent eye morphogenesis is orchestrated by neural crest cells. *Development* **132**, 4789–4800.

Meier, S. (1982) The distribution of cranial neural crest cells during ocular morphogenesis. *Prog. Clin. Biol. Res.* **82**, 1–15.

Mirzayans, F., Pearce, W.G., MacDonald, I.M. & Walter, M.A. (1995) Mutation of PAX6 gene in patients with autosomal dominant keratitis. *Am. J. Hum. Genet.* **57**, 539–548.

Nagase, T., Nakamura, S., Harii, K. & Osumi, N. (2001) Ectopically localized HNK-1 epitope perturbs migration of the midbrain neural crest cells in Pax6 mutant rat. *Dev. Growth Differ.* **43**, 683–692.

Nakamura, H. (1982) Mesenchymal derivatives from the neural crest. *Arch. Histol. Jpn.* **45**, 127–138.

Nishida, K., Kinoshita, S., Ohashi, Y., Kuwayama, Y. & Yamamoto, S. (1995) Ocular surface abnormalities in aniridia. *Am. J. Ophthalmol.* **120**, 368–375.

Osborne, N.J., Begbie, J., Chilton, J.K., Schmidt, B.J. & Eickholt, B.J. (2005) Semaphorin/neuropilin signaling influences the positioning of migratory neural crest cells within the hindbrain region of the chick. *Dev. Dyn.* **232**, 939–949.

Osumi, N., Hirota, A., Ohuchi, H., *et al.* (1997) Pax-6 is involved in the specification of hindbrain motor neuron subtype. *Development* **124**, 2961–2972.

Osumi-Yamashita, N., Kuratani, S., Ninomiya, Y., *et al.* (1997) Cranial anomaly of homozygous rSey rat is associated with a defect in the migration pathway of midbrain crest cells. *Dev. Growth Differ.* **39**, 53–67.

Osumi-Yamashita, N., Ninomiya, Y., Doi, H. & Eto, K. (1994) The contribution of both forebrain and midbrain crest cells to the mesenchyme in the frontnasal mass of mouse embryos. *Dev. Biol.* **164**, 409–419.

Pietri, T., Eder, O., Blanche, M., Thiery, J.P. & Dufour, S. (2003) The human tissue plasminogen activator-Cre mouse: a new tool for targeting specifically neural crest cells and their derivatives in vivo. *Dev. Biol.* **259**, 176–187.

Prosser, J. & Van Heyningen, V. (1998) PAX6 mutations revised. *Hum. Mutat.* **11**, 93–108.

Quinn, J.C., West, J.D. & Kaufman, M.H. (1997) Genetic background effects on dental and other craniofacial abnormalities in homozygous small eye (Pax6Sey/Pax6Sey) mice. *Anat. Embryol. (Berl)* **196**, 311–321.

Ramaesh, T., Collinson, J.M., Ramaesh, K., Kaufman, M.H., West, J.D. & Dhillon, B. (2003) Corneal abnormalities in Pax6$^{-/-}$ small eye mimic human aniridia-related keratopathy. *Invest. Ophthalmol. Vis. Sci.* **44**, 1871–1878.

Ramaesh, K., Ramaesh, T., Dutton, G.N. & Dhillon, B. (2005) Evolving concepts on the pathogenic mechanisms of aniridia related keratopathy. *Int. J. Biochem. Cell Biol.* **37**, 547–557.

Serbedzija, G.N., Bronner-Fraser, M. & Fraser, S.E. (1992) Vital dye analysis of cranial neural crest cell migration in the mouse embryo. *Development* **116**, 297–307.

Smith, A., Robinson, V., Patel, K. & Wilkinson, D.G. (1997) The EphA4 and EphB1 receptor tyrosine kinases and ephrin-B2 ligand regulate target migration of branchial neural crest cells. *Curr. Biol.* **7**, 561–570.

Suemori, H., Kadodawa, Y., Goto, K., Araki, I., Kondoh, H. & Nakatsuji, N. (1990) A mouse embryonic stem cell line showing pluripotency of differentiation in early embryos and ubiquitous beta-galactosidase expression. *Cell Differ. Dev.* **29**, 181–186.

Suzuki, R., Shintani, T., Sakuta, H., *et al.* (2000) Identification of RALDH-3, a novel retinaldehyde dehydrogenase expressed in the ventral region of the retina. *Mech. Dev.* **98**, 37–50.

Tomita, Y., Matsumura, K., Wakamatsu, Y., *et al.* (2005) Cardiac neural crest cells contribute to the dormant multipotent stem cell in the mammalian heart. *J. Cell Biol.* **170**, 1135–1146.

Ton, C.C., Hirvonen, H., Miwa, H., *et al.* (1991) Positional cloning and characterization of a paired box- and homeobox-containing gene from the aniridia region. *Cell* **67**, 1059–1074.

Trainor, P.A. & Tam, P.P. (1995) Cranial paraxial mesoderm and neural crest cells of the mouse embryo: co-contribution in the craniofacial mesenchyme but distinct segregation in branchial arches. *Development* **121**, 2569–2582.

Twigg, S.R., Kan, R., Babbs, C., *et al.* (2004) Mutations of ephrin-B1 (EFNB1), a marker of tissue boundary formation, cause craniofrontnasal syndrome. *Proc. Natl. Acad. Sci. USA* **101**, 8652–8657.

Vincent, M.C., Pujo, A.L., Olivier, D. & Calvas, P. (2003) Screening for PAX6 gene mutations is consistent with haploinsufficiency as the main mechanism leading to various ocular defects. *Eur. J. Hum. Genet.* **11**, 163–169.

Yamauchi, Y., Abe, K., Mantani, A., *et al.* (1999) A novel transgenic technique that allows specific marking of the neural crest cell lineage in mice. *Dev. Biol.* **212**, 191–203.

Yamazaki, H., Sakata, E., Yamane, T., *et al.* (2005) Presence and distribution of neural crest-derived cells in the murine developing thymus and their potential for differentiation. *Int. Immunol.* **17**, 549–558.

Yu, H.H. & Moens, C.B. (2005) Semaphorin signaling guides cranial neural crest cell migration in zebrafish. *Dev. Biol.* **280**, 373–385.

Received: 24 November 2005
Accepted: 10 May 2006

J. Biochem. **140**, 793–798 (2006)
doi:10.1093/jb/mvj208

Negative Selection with the *Diphtheria toxin A fragment* Gene Improves Frequency of Cre-Mediated Cassette Exchange in ES Cells

Kimi Araki[1,*], Masatake Araki[2] and Ken-ichi Yamamura[1]
[1]Department of Developmental Genetics, Institute of Molecular Embryology and Genetics, and [2]Institute of Resource Development and Analysis, Kumamoto University, Honjo 2-2-1, Kumamoto 860-0811

Received August 12, 2006; accepted October 11, 2006

The Cre-*lox* system is an important tool for genetic manipulation in embryonic stem cells. We previously reported that the cassette exchange strategy using the mutant *lox*66/71 and *lox*2272 combination showed high recombination efficiency and stability. However, the efficiency was strongly affected by the position of chromosomal target *lox* sites. To enrich successful cassette exchange events, even in clones showing lower recombination efficiency, we have improved exchange vector. The *Diphtheria toxin A fragment* gene was placed in the un-exchanged region for negative selection and the *puromycin N-acetyltransferase* gene, instead of the *neomycin phosphotransferase* gene, was used for positive selection. By reducing random integration, the frequency of successful cassette exchange increased up to 2–4 fold. Furthermore, by adding the third *lox* site to induce intrarmolecular recombination, the recombination efficiency of cassette exchange itself was improved, and the frequency increased to maximum 5 fold, in which the percentage of exchanged clones reached to 50–70%. This strategy should be useful for other recombinase-mediated cassette exchanges.

Key words: cassette exchange, Cre recombinase, *Diphtheria toxin A fragment* (*DT-A*) gene, embryonic stem (ES) cells, site-directed recombination.

Abbreviations: bsr, blasticidin S resistant; DT-A, diphtheria toxin A fragment; ES, embryonic stem; neo, neomycin phosphotransferase; NLSLacZ, *lacZ* gene fused with the nuclear localizing signal, pA, polyadenylation; pac, puromycin *N*-acetyltransferase; Pgk, phosphoglycerate kinase-1; RMCE, Recombinase Mediated Cassette Exchange; tk, thymidine kinase; X-gal, 5-bromo-4-chloro-3-indolyl β-D-galactopyranoside.

The Cre-mediated site-specific targeting system is a powerful tool for genome engineering in mammals, especially in mouse embryonic stem (ES) cells, because it allows precise and repeated knock-ins of any DNA to target *lox* sites introduced by gene targeting or gene trapping. (*1–3*) However, intermolecular recombination between wild-type *lox*P sites, *i.e.*, integrative recombination, is inefficient due to re-excision through intramolecular recombination (*4*).

In order to perform Cre-mediated insertion or replacement, two kinds of mutant *lox* sites have been developed. One is a pair of *lox* sites with a 5 bp mutation in the left or right end of the *lox* sequence, such as *lox*66/71 (*5*, *6*). Recombination between a chromosomally located *lox*71 site and a *lox*66 site on a targeting plasmid results in site-specific integration of the plasmid producing a double mutant *lox* site at both ends and a wild-type *lox*P site. Since the binding affinity of the double *lox* mutant site for Cre recombinase is reduced, the integrated plasmid is stably retained. The other mutant site is a heterospecific *lox* site that has mutation(s) in the central 8 bp spacer region (*7–9*). The recombination using heterospecific *lox* sites is termed Recombinase Mediated Cassette Exchange (RMCE) (*10*), in which the recombination does not occur between two *lox* sites differing in the spacer region whereas *lox* sites with identical spacer regions can be recombined efficiently. Until now, *lox*511 (*11*), *lox*2272 (*12*) and *lox*5171 (*13*) have been successfully used in ES cells.

Recently, we have shown that the combination of *lox* 66/71 and the heterospecific *lox*2272 site gave high recombination efficiency and stability even with Cre recombinase (*14*), and developed an exchangeable gene trap vector carrying *lox*71, *lox*P and *lox*2272 (*3*). Using the trap vector, we can initially carry out random insertional mutagenesis in ES cells, and then replace the reporter gene in the trap vector with any gene of interest to be expressed under the control of the trapped promoter through RMCE.

In RMCE, a targeting plasmid carrying an integrated floxed cassette is co-electroporated with a Cre-expression vector into cells in their circular forms to reduce random integration. However, random integration of targeting plasmid also occurs at a considerable frequency, probably due to nicks in plasmid DNA strands. In our previous study, the percentage of random integrants was over 50% even in the clone that showed the highest RMCE frequency, indicating that random integration is more efficient than RMCE. The most effective method to eliminate random integrants is negative selection using the *thymidine kinase* (*tk*) gene of the Herpes simplex virus (*15*). In this method, the *tk* gene is placed on a chromosomal target construct between two heterospecific *lox* sites, and recombined clones, where the *tk* gene should be removed by

*To whom correspondence should be addressed. E-mail: arakimi@gpo.kumamoto-u.ac.jp

replacement with other DNA on the targeting vector, are selected with ganciclovir. Several groups reported that almost all clones obtained after electroporation had targeted replacement (*12*, *16*, *17*). This *tk* negative selection is very useful because it is not necessary to have any positive marker on targeting vectors. On the other hand, the necessity of placing the *tk* gene in a chromosomal target construct is quite inconvenient for gene trapping, since it is preferable that trap vectors should consist of minimum elements to avoid unexpected effect(s) caused by introduction of vector elements. Actually, male sterility caused by ectopic expression of the *tk* gene in testis has been reported (*18*).

In this study, we aimed to increase recombination frequency by improving exchange vectors, not chromosomal target constructs. We used the *Diphtheria toxin A fragment* (*DT-A*) gene (*19*) for negative selection to reduce random integrants, changed the *neomycin phosphotransferase* (*neo*) gene into the *puromycin N-acetyltransferase* (*pac*) gene, and added a *lox*66 site to induce intra-molecular recombination within the exchange vector. With the improved exchange vector, the frequency of exchanged clones was increased to 2–5 folds.

MATERIALS AND METHODS

Plasmids—Plasmids p66-2272 and pCAGGS-Cre were described previously (*14*, *20*). The plasmid containing the MC1 promoter–DT-A gene was kindly provided by Dr. S. Aizawa (*19*). However, The original MC1-DT-A cassette had no polyadenylation (pA) signal and the MC1 promoter of the cassette carried only one copy of the enhancer sequence. The MC1-DT-A-pA cassette used in this study was constructed by replacing the original promoter by the MC1 promoter from MC1-neo-pA cassette (STRATAGENE, La Jolla, USA) and by adding the pA signal of the rabbit β-grobin gene. The pMC1-DTA plasmid was constructed by inserting the MC1-DT-A-pA cassette into p66-2272. The pPGK-DTA and pPac-DTA were constructed by replacing the MC1-neo-pA cassette into the Pgk-neo-pA and Pgk-pac-pA cassette, respectively. The pPac-DTA-66 was constructed by inserting a *lox*66 fragment into pPac-DTA. The sequences of all *lox* sites in these plasmids were confirmed by DNA sequencing.

Cell Culture and Electroporation—ES cell culture and establishment of cell lines carrying a single copy of target *lox* sites was described previously (*14*). For RMCE, the cells ($3–6 \times 10^6$ cells/0.8 ml in PBS) were electroporated at 400 V and 125 μF, and plated into two 10 cm plates. G418 selection was started after 24 h of electroporation at 200 μg/ml for 7 days. For puromycin selection, cells were fed 2 μg/ml of puromycin containing medium for 24 h × 2 times on day 1 and 4 after electroporation. On day 8, colonies were stained with 5-bromo-4-chloro-3-indolyl β-D-galactopyranoside (X-gal) or picked and expanded for DNA analysis.

A series of 5 exchange vectors with a cell line was performed on the same day, and each series of electroporation was repeated at least four times on independent days.

PCR Analysis—Genomic DNA (0.05–0.1 μg) was subjected to 32 cycles of amplification (each cycle consisted of 1 min at 94°C, 1.5 min at 58°C and 1.5 min at 72°C) using AmpliTaq polymerase (Perkin-Elmer). Primer sequences are as follows; AG2, 5′-CTGCTAACCATGTTCATGCC-3′; LZUS3, 5′-GCGCATCGTAACCGTGCAT-3′; bsr-2, 5′-GCAGAAATCGGAGGAAGAAG-3′; bsr-3, 5′-CAACTCCCTACACATACCAC-3′; FRT-S, 5′-GCTTCAAAAGCGCTCTGAAG-3′; DTA1, 5′-TACCACGGGACTAAACCTGG-3′; DTA2, 5′-CGCTTAACGCTTTCGCCTGT-3′.

Statistical Analyses—The recombination efficiencies and relative number of blue or white colonies were evaluated by non-repeated measures ANOVA. Where a significant difference ($p < 0.05$) was identified, the differences were analyzed further with SNK tests for multiple comparisons.

RESULTS

Experimental Design—The strategy to assess the RMCE frequencies used previously (*14*) is outlined in Fig. 1A. The chromosomal target is the CAG promoter-*lox*71-*Blasticidin S resistant* (*bsr*) gene-pA-*lox*511-FRT-*lox*2272. Exchange vectors contain *lox*66-the promoter-less *lacZ* gene fused with the nuclear localizing signal (*NLSlacZ*)-a selection marker gene-*lox*2272. ES cell lines carrying the chromosomal target are co-electroporated with the exchange vector and Cre-expression vector in their circular forms, and then selected with appropriate drug according to the selection marker gene. The *cre* gene on the expression vector is transiently expressed, and Cre protein mediates site-specific recombination between the chromosomal *lox*71 and *lox*66 on the targeting plasmid, and the chromosomal *lox*2272 and *lox*2272 on the targeting plasmid, resulting in cassette exchange of the *bsr* gene with the *NLSlacZ*-selection marker cassette. Since there is no negative selection marker on the chromosomal target construct, both random integrants and site-specific recombinants become drug resistant, but only the colonies where RMCE had occurred are stained blue with X-gal, since the *NLSLacZ* gene is inserted downstream of the CAG promoter. The percentage of blue colonies represents the frequency of RMCE. When only the exchange vector was electroporated, no blue colonies appeared (data not shown), indicating that gene trapping events hardly occur with electroporation using the exchange vectors in circular forms.

We used four ES cell lines, 71-5F2-7, 71-5F2-10, 71-5F2-23 and 71-5F2-26 carrying a single copy of the chromosomal target construct. The cell lines 71-5F2-10 and 71-5F2-23 were used in our previous study (*14*), and showed lower and higher recombination frequency, respectively. We added two cell lines, 71-5F2-7 and 71-5F2-26, which showed lower recombination frequency, to examine enrichment effects of exchange vectors on several different "inactive" positions. Since the original 71-5F2-7, 71-5F2-10 and 71-5F2-26 clones were contaminated with wild-type ES cells at a considerable percentage (data not shown), all four lines were re-cloned through limiting dilution and Blasticidin S selection. Table 1 shows the RMCE frequencies and the number of blue colonies in each re-cloned line electroporated with pCAGGS-Cre and p66-2272, which contains only the MC1-*neo*-pA cassette as a positive selection marker (Fig. 1B, top) and gave the best frequency in the previous study. Since the conditions of electroporation were optimized for Cre-mediated recombination, the frequency in 71-5F2-23 increased to 35.3% from the frequency obtained in the previous study, 26.3%. In 71-5F2-23, the number of blue colonies was 3–4 times higher than in the

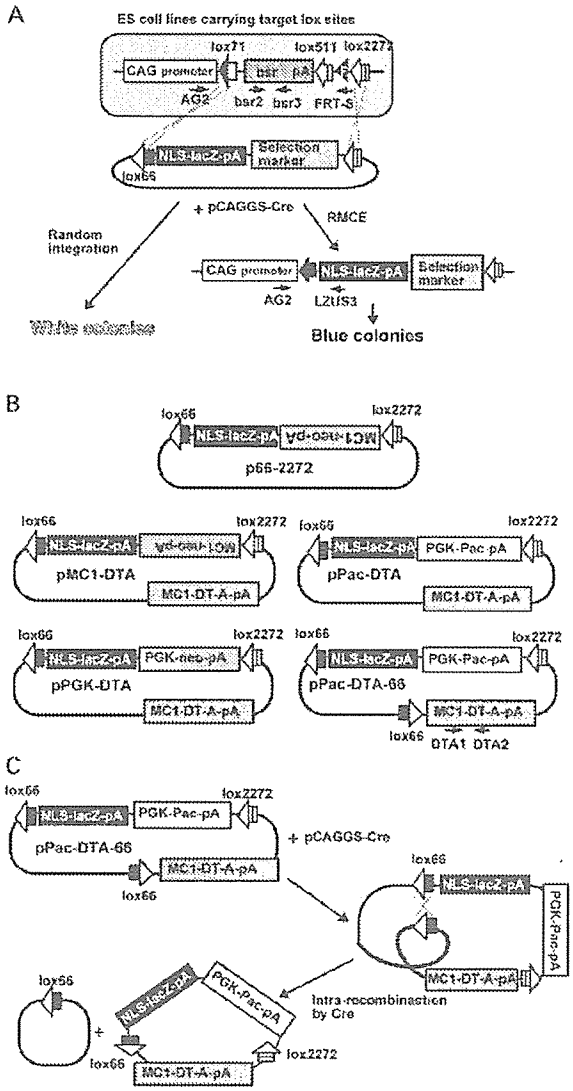

Fig. 1. **(A) Experimental strategy for comparison of frequency of RMCE.** ES cell lines carrying a single copy of the CAG-*lox*71-bsr-pA-*lox*511-FRT-*lox*2272 fragment were established. The cell lines were co-electroporated with the Cre expression vector and the targeting plasmids carrying the promoter-less *NLS-lacZ* gene. Through RMCE, the *NLSlacZ* gene is joined to the CAG promoter, resulting in positive staining with X-gal. Since the targeting plasmids contain a selection marker gene, random integrants can also appear. However, colonies with random integration are not stained because there is no promoter for the *NLSlacZ* gene. The percentage of blue colonies represents the frequency of RMCE. Positions of PCR primers used in Table 2 are shown as small arrows with the name of the primer. **(B) Targeting vectors used in this study. (C) Predicted recombination intermediate of pPac-DTA-66.** Since pPac-DTA-66 carries two *lox*66 sites, intra-molecular recombination should occur first to divide into two circular molecules. The molecule including *lox*66 and *lox*2272 becomes a substrate of RMCE.

other three clones, indicating high recombination efficiency probably due to open chromosomal configuration around the target *lox* sites. The goal of this study is to improve targeting vectors to enrich blue colonies in all cell lines, including the "lower" recombination-frequency clones.

Table 1. **Recombination frequency with p66-2272 targeting vector in clones used in this study.**

Cell line	Number of Blue colonies ± SD	Recombination Frequency (%) ± SD
71-5F2-7	121 ± 29.6	20.2 ± 5.89
71-5F2-10	92.0 ± 34.6	16.5 ± 2.67
71-5F2-23	311 ± 166	35.3 ± 7.89
71-5F2-26	67.0 ± 17.8	11.6 ± 2.44

$N = 4$ in each clone.

Exchange Vectors—Exchange vectors used in this study are shown in Fig. 1B. In pMC1-DTA, we added the MC1 promoter-*DT-A* gene-pA cassette to p66-2272 in the un-integrated region by RMCE (outside of two *lox* sites) for negative selection to reduce random integrants. The choice of selection marker gene is also important for colony formation efficiency. In pPGK-DTA, the mouse *phosphoglycerate kinase-1* (*Pgk*) promoter–*neo*-pA cassette, which shows higher colony efficiency than MC1-neo, is used, and in pPac-DTA, the *Pgk* promoter–*pac*-pA cassette, which is known to that puromycin sensitive cells are killed quite quickly and the drug selection completes within 24–48 h, is used. In addition, we constructed a pPac-DTA-66 plasmid, in which an additional *lox*66 site was placed between the DT-A cassette and plasmid vector sequence. After electroporation with Cre expression plasmid, intra-molecular recombination between *lox*66 sites should take place first, resulting in two circular molecules as shown Fig. 1C. By minimizing the size of the targeting DNA molecule, we expected to reduce random integration.

Recombination Frequencies—Percentages of blue colonies, *i.e.*, RMCE frequencies, in the 4 lines are shown in Fig. 2A. The pPac-DTA-66 plasmid (vector no. 5) gave the highest RMCE frequency in all lines with statistical significant differences. Even in the 'lower' recombination-frequency clone 71-5F2-26, the frequency exceeded 50%, and in the "high" recombination-frequency clone 71-5F2-23 line, it reached to 75%. In order to evaluate the enrichment effect, relative numbers of blue or white colonies against the number of blue colonies obtained with p66-2272 were calculated and are shown in Fig. 2B. When the DT-A cassette was added to p66-2272 (pMC1-DTA), the number of white colonies was significantly reduced to almost half (vector no. 2), indicating that negative selection of the DT-A was effective. However, since the number of blue colonies was also slightly reduced, the percentages of blue colonies did not change significantly, but were higher than in p66-2272. With the use of the PGK-neo-pA, both the number of blue and white colonies increased, but no significant changes of frequency compared to pMC1-DTA observed (vector no. 3).With the use of PGK-pac-pA, the RMCE frequency increased to 30–50% (vector no. 4). Interestingly, with pPac-DTA-66 plasmid, the numbers of blue colonies (targeted integration) were significantly increased in all lines, whereas the numbers of white colonies (random integration) were unchanged (vector no. 5). This indicates that smaller DNA molecule can access more easily to chromosomal target *lox* sites.

In order to analyze integration patterns, 71-5F2-7 and 71-5F2-10 colonies were picked from cells electroporated

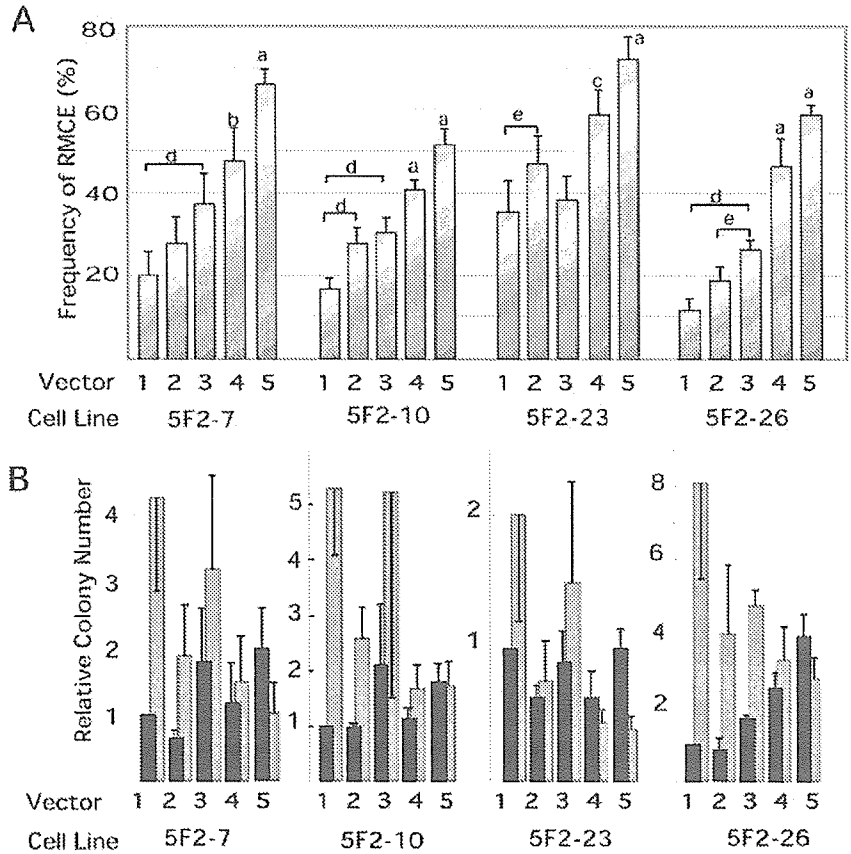

Fig. 2. **(A) Frequency of RMCE.** Twenty micrograms of each replacement plasmid and the Cre-expressing vector were co-electroporated, and after drug selection for 7 days, colonies were stained with X-gal, and the percentage of positive colonies was scored as the frequency of RMCE. Numbers under the graph indicate the targeting vector used in each electroporation. 1, p66-2272; 2, pMC1-DTA; 3, pPGK-DTA; 4, pPac-DTA, 5, pPac-DTA-66. The means ± SD of at least four independent electroporations are represented. All cell lines show significant differences at $P < 0.01$ by ANOVA analysis. Statistical significances among vectors were further analyzed by the SNK test. a, $P < 0.01$ compared to all other vectors; b, $P < 0.01$ compared to vector 1, 2 and 5 and $P < 0.05$ compared to vector 3; c, $P < 0.01$ compared to vector 1, 3 and 5 and $P < 0.05$ compared to vector 2; d, $P < 0.01$ compared to the indicated vector; e, $P < 0.05$ compared to the indicated vector. **(B) Relative Blue (solid bars) or white (gray bars) colony numbers.** The number of blue colonies obtained with p66-2272 arbitrarily set at 1.

Table 2. **Genomic DNA analysis of isolated subclones by PCR.**

Cell line	Total no. of clones analyzed	X-Gal staining (%)	PCR pimers			
			AG2/LZUS3	bsr2/bsr3	AG2/FRT-AS	DTA1/DTA2
71-5F2-7	18	Blue 8 (44)	8	0	ND	0
		White 10 (56)	0	5	5	2
71-5F2-10	23	Blue 14 (61)	14	0	ND	0
		White 9 (39)	0	6	3	0

Subclones obtained after coelectroporation with pPac-DTA-66 and pCAGGS-Cre were picked and expanded for genomic DNA preparation and PCR analysis. Part of each clone was stained with X-gal, and the number of blue or white clones is represented. PCR analyses were performed with the indicated primers (see Fig. 1), and among the each blue or white clones, the number of clones showed a band of expected size is represented. ND, not done.

with pPac-DTA-66 and pCAGGS-Cre, genomic DNAs were prepared, and PCR analysis was performed. As shown in Fig. 1A, the 5′-junction of the recombination can be amplified using the primers AG2 and LZUS3, and all blue clones gave a band of the expected size (Table 2, data of electrophoresis not shown). Then, the presence of the *bsr* gene, which should be removed through RMCE, was examined with the primers bsr-1 and bsr-2. All blue clones were negative for the *bsr* gene detecting PCR, however, only 11 clones out of 19 white clones retained the bsr gene, unexpectedly. Since it is reported that *lox*511 can be recombined with *lox*P or *lox*71 (*9*), PCR analysis with AG2 and FRT-AS primers was performed to detect recombination between *lox*71 and *lox*511. The 8 clones that did not carry the *bsr* gene exhibited a 201-bp band. We cloned the product into the T-vector and confirmed that the sequence corresponded to the recombination product *lox*71 and *lox*511. The spacer sequence of the *lox* site in the recombined product was the wild-type sequence (data not shown). The *DT-A* gene was detected in only 2 clones by PCR, indicating successful negative selection. Since the amplified region was the inside of the ORF, the promoter or pA signal might be deleted in these 2 clones.

DISCUSSION

We have shown here that the combined usage of negative selection of the *DT-A* gene, positive selection of the *Pac* gene and the third *lox* site for intra-molecular recombination efficiently enriched RMCE events. The enrichment

effect was more apparent in the 'lower' recombination-frequency clones, and we could obtain a frequency of 50% and more, which is high enough for the practical use of RMCE.

We could enrich RMCE event through two strategies, one is the use of the *DT-A* negative selection marker gene and the other is the change of positive selection marker gene. The usefulness of the *DT-A* gene which reduce random integration has been already reported in gene targeting (*21*), however, enrichment effect in gene targeting frequency by changing selection marker has not been clearly observed. In comparing two plasmids having the same promoter, pPac-DTA (Pgk-Pac) and pPGK-DTA (Pgk-neo), the number of white colonies was reduced to almost half, probably due to the difference of colony formation efficiency of the *pac* and *neo* gene. On the other hand, in comparison between pMC1-DTA (MC1-neo) and pPac-DTA (Pgk-pac), there is no statistical difference in number of white colonies or blue colonies, except of blue colonies in 71-5F2-26, nevertheless, the RMCE frequency showed statistical difference in the all lines used in this experiment. Why the use of the Pgk-*pac* cassete resulted in higher RMCE frequency? We speculate that the difference of time course in G418 and puromycin selection might be the cause of the enrichment effect. Puromycin kills almost all sensitive cells within 24hrs, whereas G418 takes 2–3 days. The quick elimination of non-transfected cells might result in reduction of spontaneously drug-resistant colonies.

In addition to reduction of random integration, we could increase recombination efficiency itself by adding the third *lox* site to induce intra-molecular recombination, which results in 33% of size reduction of targeting DNA molecule by removal of the plasmid vector sequence. Interestingly, the numbers of blue colonies with pPac-DTA-lox66 plasmid were 1.5–1.7 times higher than those with pPac-DTA plasmid, thus, the RMCE efficiencies increase approximately in inverse proportion with the size of targeting DNA molecule. This indicates that the probability of encounter of chromosomal *lox* site and targeting plasmid depends on physical mobility of DNA molecule. In the higher-recombination efficiency clone 71-5F2-23, the chromosomal configuration around *lox* sites is considered to be open, therefore, they always show high efficiency even when the molecular weight of targeting vector is relatively large. On the other hand, in the lower-recombination efficiency clone 71-5F2-26, the chromosomal configuration around *lox* sites is considered to be close, therefore, reduction of the molecular weight of targeting DNA is quite effective to increase RMCE frequency by improving accessibility to chromosomal target *lox* sites. Our results predict that RMCE using large molecular weight plasmid, *ex.* bacterial artificial chromosome, may show low frequency.

The advantage of RMCE using our strategy is the minimum requirement of the chromosomal target structure, *i.e.*, only two heterospecific *lox* sites, and wide and easy application to gene targeting or gene trapping vectors. Thus, our enrichment strategy for RMCE will be a powerful tool in genetic manipulation in ES cells.

We wish to thank Ms. K. Haruna, M. Muta, R. Minato and Y. Tsuruta for technical assistance. This work was supported in part by a Grant-in-Aid on Priority Areas from the Ministry of Education, Science, Culture and Sports of Japan, by a grant from the Osaka Foundation for Promotion of Clinical Immunology.

REFERENCES

1. Nagy, A. (2000) Cre recombinase: the universal reagent for genome tailoring. *Genesis* **26**, 99–109
2. Branda, C.S. and Dymecki, S.M. (2004) Talking about a revolution: The impact of site-specific recombinases on genetic analyses in mice. *Dev. Cell* **6**, 7–28
3. Taniwaki, T., Haruna, K., Nakamura, H., Sekimoto, T., Oike, Y., Imaizumi, T., Saito, F., Muta, M., Soejima, Y., Utoh, A., Nakagata, N., Araki, M., Yamamura, K., andAraki, K. (2005) Characterization of an exchangeable gene trap using pU-17 carrying a stop codon-β *geo* cassette. *Dev. Growth Differ.* **47**, 163–72
4. Fukushige, S. and Sauer, B. (1992) Genomic targeting with a positive-selection lox integration vector allows highly reproducible gene expression in mammalian cells. *Proc. Natl. Acad. Sci. USA* **89**, 7905–9
5. Albert, H., Dale, E.C., Lee, E., and Ow, D.W. (1995) Site-specific integration of DNA into wild-type and mutant lox sites placed in the plant genome. *Plant J.* **7**, 649–59
6. Araki, K., Araki, M., and Yamamura, K. (1997) Targeted integration of DNA using mutant lox sites in embryonic stem cells. *Nucleic Acids Res.* **25**, 868–72
7. Hoess, R.H., Wierzbicki, A., and Abremski, K. (1986) The role of the loxP spacer region in P1 site-specific recombination. *Nucleic Acids Res.* **14**, 2287–300
8. Lee, G. and Saito, I. (1998) Role of nucleotide sequences of loxP spacer region in Cre-mediated recombination. *Gene* **216**, 55–65
9. Langer, S.J., Ghafoori, A.P., Byrd, M., and Leinwand, L. (2002) A genetic screen identifies novel non-compatible loxP sites. *Nucleic Acids Res.* **30**, 3067–77
10. Bouhassira, E.E., Westerman, K., and Leboulch, P. (1997) Transcriptional behavior of LCR enhancer elements integrated at the same chromosomal locus by recombinase-mediated cassette exchange. *Blood* **90**, 3332–44
11. Bethke, B. and Sauer, B. (1997) Segmental genomic replacement by Cre-mediated recombination: genotoxic stress activation of the p53 promoter in single-copy transformants. *Nucleic Acids Res.* **25**, 2828–34
12. Kolb, A.F. (2001) Selection-marker-free modification of the murine beta-casein gene using a lox2272 [correction of lox2722] site. *Anal. Biochem.* **290**, 260–71
13. Osipovich, A.B., Singh, A., and Ruley, H.E. (2005) Post-entrapment genome engineering: first exon size does not affect the expression of fusion transcripts generated by gene entrapment. *Genome Res.* **15**, 428–35
14. Araki, K., Araki, M., and Yamamura, K. (2002) Site-directed integration of the cre gene mediated by Cre recombinase using a combination of mutant lox sites. *Nucleic Acids Res.* **30**, e103
15. Seibler, J., Schubeler, D., Fiering, S., Groudine, M. and,Bode, J. (1998) DNA cassette exchange in ES cells mediated by Flp recombinase: an efficient strategy for repeated modification of tagged loci by marker-free constructs. *Biochemistry* **37**, 6229–34
16. Soukharev, S., Miller, J.L., and Sauer, B. (1999) Segmental genomic replacement in embryonic stem cells by double lox targeting. *Nucleic Acids Res.* **27**, e21
17. Shmerling, D., Danzer, C.P., Mao, X., Boisclair, J., Haffner, M., Lemaistre, M., Schuler, V., Kaeslin, E., Korn, R., Burki, K., Ledermann, B., Kinzel, B., and Muller, M. (2005) Strong and ubiquitous expression of transgenes targeted into the beta-actin locus by Cre/lox cassette replacement. *Genesis* **42**, 229–35

18. al-Shawi, R., Burke, J., Wallace, H., Jones, C., Harrison, S., Buxton, D., Maley, S., Chandley, A. andBishop, J.O. (1991) The herpes simplex virus type 1 thymidine kinase is expressed in the testes of transgenic mice under the control of a cryptic promoter. *Mol. Cell. Biol.* **11**, 4207–16
19. Yagi, T., Nada, S., Watanabe, N., Tamemoto, H., Kohmura, N., Ikawa, Y. andAizawa, S. (1993) A novel negative selection for homologous recombinants using diphtheria toxin A fragment gene. *Anal. Biochem.* **214**, 77–86
20. Araki, K., Imaizumi, T., Okuyama, K., Oike, Y., and Yamamura, K. (1997) Efficiency of recombination by Cre transient expression in embryonic stem cells: comparison of various promoters. *J. Biochem.* **122**, 977–82
21. Yanagawa, Y., Kobayashi, T., Ohnishi, M., Tamura, S., Tsuzuki, T., Sanbo, M., Yagi, T., Tashiro, F., and Miyazaki, J. (1999) Enrichment and efficient screening of ES cells containing a targeted mutation: the use of DT-A gene with the polyadenylation signal as a negative selection maker. *Transgenic Res.* **8**, 215–21

骨の解剖(構造)と生理

東京大学大学院医学系研究科感覚・運動機能医学整形外科講師　田中　栄

骨を理解するのためのKEY phrase

①骨組織は基質蛋白質とミネラルから構成される。
②骨形成は骨芽細胞，骨吸収は破骨細胞によって担われる。
③骨リモデリングは骨芽細胞・破骨細胞が相互に関与しながら働く骨組織の恒常性維持機構である。

骨の解剖(構造)

骨組織

◆骨組織は基質蛋白質とハイドロキシアパタイトを中心とした骨ミネラル，そしてそれらの産生・代謝に携わるさまざまな細胞から構成されている。基質蛋白質の大部分はⅠ型コラーゲンによって占められ，非コラーゲン性蛋白質としてはオステオカルシンなどが存在する。

◀ 骨組織は基質蛋白質，骨ミネラル，細胞から成る。

◆骨形成は主として骨芽細胞，骨吸収は破骨細胞が担っており，骨基質のなかで互いに密なネットワークを張りめぐらせている骨細胞は，メカニカルストレスのセンサーとして働くと考えられている。

◆副甲状腺で産生される上皮小体ホルモン(PTH)は骨芽細胞に作用し，骨形成を促進する。甲状腺C細胞で産生されるカルシトニンは破骨細胞に作用し，骨吸収を抑制する。

骨の生理

骨リモデリング

◆骨組織は身体の形状を保ち，臓器を保護するのみならず，体内最大のカルシウム貯蔵庫として生体の恒常性維持にも重要な役割を果たしている。このような機能を果たすために，骨組織では成長が終わった後も，破骨細胞による骨吸収(によるカルシウムの放出)とそれに引き続く骨芽細胞による骨形成が相互に関与しながら間断なく行われており，この過程は「骨リモデリング」とよばれる。

◀ 骨組織では，破骨細胞による骨吸収と骨芽細胞による骨形成が常に行われている(骨リモデリング)。

◆リモデリングは休止相→活性化相→吸収相→逆転相→形成相→休止相という一連のサイクルで行われている。

◆休止状態にある骨表面(休止相)に何らかの刺激が加わると破骨細胞分化が誘導され(活性化相)，骨吸収が進行する(吸収相)。吸収を終えると破骨細胞はアポトーシスによって消失し，骨芽細胞分化が誘導される(逆転相)。骨芽細胞が破壊された骨を補うように骨形成を開始し(形成相)，一定量の骨が形成されると再び骨表面は休止相になる。同様の吸収→形成サイクルは骨折治癒の過程でも観察される。

◆リモデリングの場であるひとつのbasic multicellular unit(BMU)において，骨吸収の開始から骨形成の終了まで，という一つのリモデリングサイクルが完成するには，ヒトの場合6カ月から9カ月を要するが，注目すべきは，骨形成相が約3カ月であるのに対し，吸収相は約2週間と短いことである(**図1**)。このため骨リモデリングは，「骨量」維持に関しては基本的にはネガティブな過程であり，骨粗鬆症などにおいてリモデリングの亢進は骨量減少に関するリスクファクターであると考えられている。しかしながら，骨壊死などでリモデリ

◀ヒトのリモデリングサイクルの周期は6カ月～9カ月。そのうち骨形成相が約3カ月，骨吸収相は約2週間である。

図1　骨リモデリングの概念

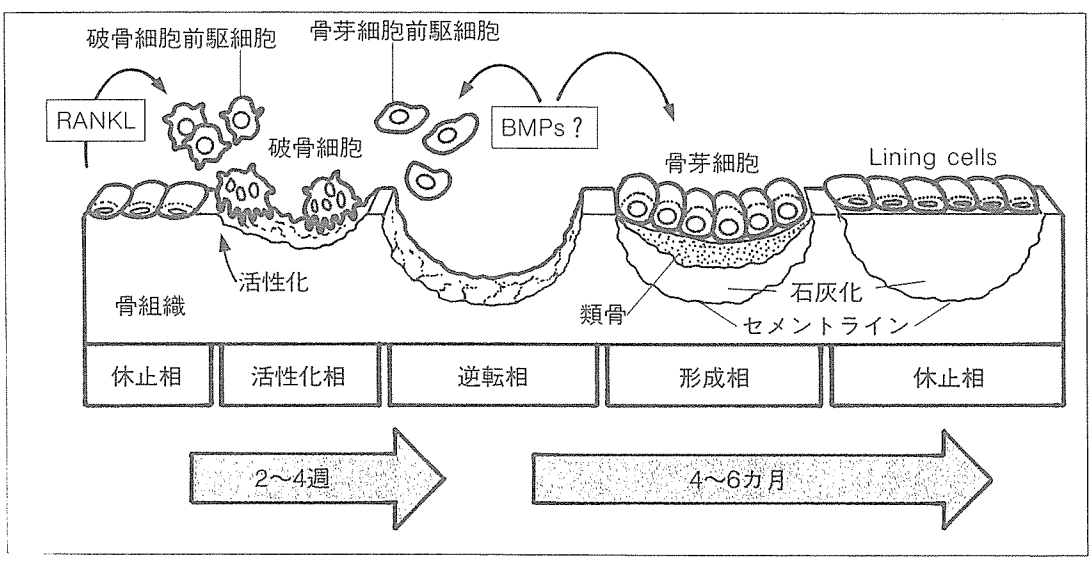

(文献1より改変)

図2　リモデリングの頻度と骨強度との関係

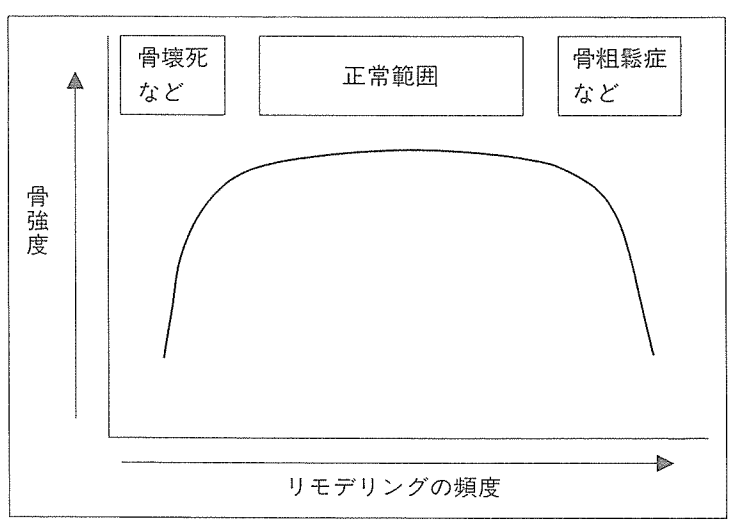

(文献2より一部改変)

ングが著しく低下した骨組織では劣化が進むため，長期的には強度が減弱する。すなわち骨の健全性を保つためには，リモデリングサイクルを適切なレベルで維持することが重要である(図2)。

◆現在，骨粗鬆症治療として用いられている骨吸収抑制剤は，破骨細胞による骨吸収を抑制し，リモデリングサイクルを低下させる。

◎文献

1) Riggs BL, Parfitt AM : Drugs used to treat osteoporosis : the critical need for a uniform nomenclature based on their action on bone remodeling. J Bone Miner Res, 20(2) : 177-184, 2005.
2) Weinstein RS : True strength. J Bone Miner Res, 15(4) : 621-625, 2000.

POINT UP VIEW

基礎最前線

近年骨芽細胞・破骨細胞分化の分子メカニズムがかなり詳細に明らかになってきた。破骨細胞は単球・マクロファージ系の前駆細胞から分化するが，その分化にTNF－αスーパーファミリーに属する膜結合型サイトカインであるreceptor activator of NF－κB ligand (RANKL)が必要不可欠なことが，さまざまな研究から明らかになってきた。また骨芽細胞の分化にはbone morphogenetic protein (BMP)をはじめとしたtransforming growth factor(TGF)－βファミリーの関与が示唆されているが，その下流で転写因子Runt domain transcription factor(runx)-2,Osterixが重要な役割を果たすことが明らかになっている。

口頭試問ファイナルアタック

・骨組織を構成する成分とは？　I型コラーゲンを主としたコラーゲン性蛋白質が基質蛋白質の大部分を占め，これに非コラーゲン性蛋白であるオステオカルシンなどが骨基質蛋白質を構成する。無機質としてはハイドロキシアパタイトを中心としたミネラルが骨組織の強度維持，カルシウム調節に重要な役割を果たす。

・骨組織を構成する細胞とその調節とは？　骨形成は間葉系幹細胞に由来する骨芽細胞，骨吸収は造血幹細胞に由来する破骨細胞によって担われる。これらの細胞の機能は上皮小体ホルモンやカルシトニンなどのホルモン，そしてRANKLやBMPなどのサイトカインによって調節される。

postmenopausal bone loss by strontium ranelate : the randomized, two-year, double-masked, dose-ranging, placebo-controlled PREVOS trial. Osteoporos Int 13 (12) : 925-931, 2002
13) Meunier PJ, Roux C, Seeman E, et al : The effects of strontium ranelate on the risk of vertebral fracture in women with postmenopausal osteoporosis. N Engl J Med 350 (5) : 459-468, 2004
14) Reginster JY, Seeman E, De Vernejoul MC, et al : Strontium ranelate reduces the risk of nonvertebral fractures in postmenopausal women with osteoporosis : Treatment of Peripheral Osteoporosis (TROPOS) study. J Clin Endocrinol Metab 90 (5) : 2816-2822, 2005
15) D'Haese PC, Schrooten I, Goodman WG, et al : Increased bone strontium levels in hemodialysis patients with osteomalacia. Kidney Int 57 (3) : 1107-1114, 2000
16) Oste L, Bervoets AR, Behets GJ, et al : Time-evolution and reversibility of strontium-induced osteomalacia in chronic renal failure rats. Kidney Int 67 (3) : 920-930, 2005

4．新しい治療薬
③ 抗 RANKL 抗体

骨吸収抑制剤による骨粗鬆症治療

現在の骨粗鬆症治療の中心になっているのは骨吸収抑制剤（anti-catabolic agents）である。中でもアレンドロネート，リセドロネートをはじめとしたビスホスホネート製剤は強力な骨吸収抑制効果を有し，膨大な基礎研究データの蓄積に加え，大規模かつ広範な臨床研究から，骨密度増加のみならず脊椎骨折，大腿骨頸部骨折の予防効果も確立されたという点で，過去に類をみない画期的な治療薬であり，現在ビスホスホネートをはじめとした骨吸収抑制剤を中心に据えた治療法が，骨粗鬆症治療グローバルスタンダードメソッドとして確立されようとしている。また関節リウマチやがん骨転移などにおける病的な骨破壊においてもビスホスホネートが有効であることが示されている。

しかしながら，ビスホスホネート製剤を中心とした治療にも様々な問題点が指摘されている。アレンドロネートやリセドロネートは腸管からの吸収がきわめて悪いため起床時に内服する必要があり，上部消化管障害が少なからず認められる。またビスホスホネートは破骨細胞に直接作用し，強力に骨吸収を抑制することにより骨代謝回転を低下させると考えられているが，骨組織に蓄積して効果を発揮するというビスホスホネートの特徴から，低代謝回転は薬物投与中止後も長期間にわたり持続する。このような長期に及ぶ低代謝回転の持続が骨組織にとって本当に有害ではないのかという点が，今後特に比較的若年の患者を治療する際には重要な問題になると考えられる。

実際に動物実験において，大量のビスホスホネートを投与した犬の骨組織で microcrack が認められること[1]，ビスホスホネート投与患者において治癒過程の遅延が認められること[2]などが報告されて

いる。また，ビスホスホネート投与によって生じたと考えられる「医原性」大理石骨病や顎骨骨壊死の発生も報告されている[3, 4]。現在，ビスホスホネートは老人の骨粗鬆症のみならず，骨形成不全症などの疾患に対して小児にも積極的に投与されているが，このような症例では投与期間が長期化することを鑑みると，安易な投与に警鐘をならすものとして注目されている。

RANKL/RANK/OPG 系による骨吸収調節

このような流れの中で，新しいコンセプトに基づいた治療薬の開発が進んでいる。破骨細胞は骨吸収をつかさどる唯一の細胞であり，その機能抑制が骨粗鬆症治療戦略として有効であることは，現在臨床で使用されている骨粗鬆症治療薬のほとんどが骨吸収抑制剤であることからも明瞭である。理想的な骨吸収抑制剤としては，①強力な吸収抑制効果を有するのみならず，②効果のオン・オフがはっきりしており（つまり投与中止によって効果が速やかに減弱する），③治療効果の減弱が認められないこと，そして④なるべく骨組織（の細胞）特異的に作用する安全な薬剤であることが期待される。また現代においては，⑤医療コストの削減も重要な課題である。

1990 年代後半になって破骨細胞研究においても分子生物学的アプローチが急速に進歩し，破骨細胞の分化・活性化における中心的な分子やシグナル伝達経路の解明が加速度的に進んできた。中でも 1998 年の RANKL（receptor activator of nuclear factor-κB ligand）の発見は，それ以降の骨代謝研究に大きなインパクトを与えた[5]。RANKL は元来，活性化 T 細胞に発現誘導され，樹状細胞の活性化，生存をつかさどる因子として同定された腫瘍壊死因子（TNF：tumor necrosis factor）スーパーファミリーに属する膜結合型サイトカインである。その後の研究によって，骨芽細胞や骨髄ストローマ細胞においても活性型ビタミン D_3，副甲状腺ホルモン（PTH：parathyroid hormone），プロスタグランジン，炎症性サイトカインなどの刺激によって RANKL の発現が誘導され，破骨細胞分化・活性化において中心的な役割を果たすことが明らかにされた。RANKL はマクロファージ系の前駆細胞に存在する受容体 RANK に結合することにより破骨細胞への分化を誘導する。また，RANK に対して競

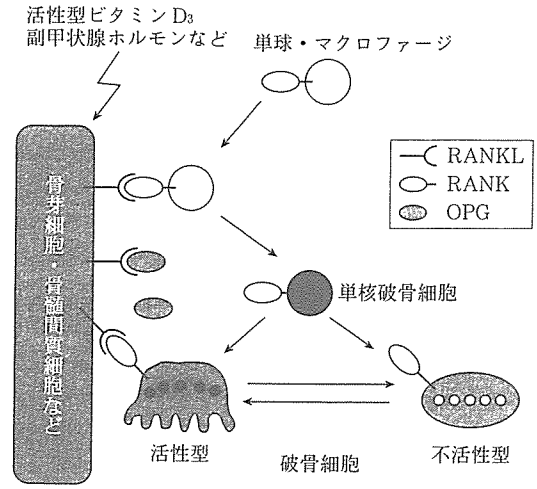

図 1　破骨細胞分化・活性化における RANKL-RANK 系の役割

OPG：osteoprotegerin，RANKL：receptor activator of nuclear factor-κB ligand

活性化ビタミン D_3 などによって骨芽細胞や骨髄間質細胞膜上に誘導された RANKL によって，破骨細胞の分化・活性化が誘導される。

合的に RANKL と結合する液性因子オステオプロテジェリン（OPG：osteoprotegerin）は，強力に破骨細胞分化を阻害する生理的なインヒビターである（図 1）。

様々な *in vitro*，*in vivo* の解析から，RANKL-RANK 系がきわめて破骨細胞分化・活性化に特異的な情報伝達系であることが明らかになった。*In vitro* においては，血球系細胞をマクロファージコロニー刺激因子（M-CSF：macrophage colony-stimulating factor）および RANKL の存在下で培養すると，破骨細胞への分化が誘導されることが証明された。また RANKL，あるいは RANK のノックアウトマウス，そして OPG の過剰発現マウスは骨吸収の低下，大理石骨病様の病態を呈し，逆に OPG のノックアウトマウス，RANKL の過剰発現マウスでは破骨細胞分化・活性化亢進による骨量減少を示す[5]。これらの結果は，RANKL-RANK 系がきわめて特

異的に破骨細胞分化・活性化にかかわっていること，すなわちRANKLが1980年代にRodan，Martinらによって提唱されていた，「骨芽細胞の産生する破骨細胞分化因子」そのものであることを示している[6]。最近，Riggsらは閉経後骨粗鬆症女性では骨髄中の間質細胞，T細胞，そしてB細胞膜表面のRANKL発現が亢進していること，それがエストロゲン治療によって低下することを明らかにしており，これはRANKLの閉経後骨粗鬆症における重要性を示唆する結果である[7]。

RANKL-RANK系をターゲットにした骨粗鬆症治療薬

これらの基礎的研究を受けて，RANKL-RANK系をターゲットにした治療薬の開発が急ピッチで進んでいる。その治療戦略としては表1のようなアプローチが試みられている。このうち最も臨床治験が進んでいるのはFc-OPGおよび抗RANKL抗体である。

OPGはTNF受容体ファミリーに属するが，他のファミリーと異なり，膜貫通ドメインをもたず，可溶型タンパクとして存在する。OPGはRANKLと特異的に結合し，RANKL-RANKの結合を阻害することによって破骨細胞分化・活性化を抑制する。このような作

表1　抗RANKL治療薬

OPG，Fc-OPG
RANK-Fc
Anti-RANKL monoclonal antibody (denosumab)
OPG-like peptidemimetics (OP3-4)
RANKL vaccine
Interferon-β，γ
p38 inhibitor (SB203580，FR167653)
JNK inhibitor (SP600125)
IKK inhibitor (NBD peptide)
NF-κB inhibitor (NF-κB decoy)
Calcineurin inhibitor (cyclosporin A，FK506)
NFAT inhibitor (VIVIT peptide)
PI3K inhibitor (wortmannin，LY290442)

用機序からOPGの骨代謝性疾患への治療応用が期待されており，動物実験においてはリコンビナントOPGもしくはイムノグロブリンFc領域とOPGとの融合タンパク投与，あるいはアデノウイルスを用いたOPG発現によって，卵巣摘出による骨粗鬆症，関節炎による骨破壊，歯周病による骨吸収，がん骨転移による骨破壊などの病的な骨破壊が抑制されることが報告されている。Amgen社はリコンビナントFc-OPG融合タンパクを作成し，閉経後骨粗鬆症患者に対する治療効果を検討し，短期的な成績ではFc-OPGが閉経後骨粗鬆症患者の骨吸収マーカーを減少させることを報告した[8]。また，多発性骨髄腫および乳がん骨転移患者に対するFc-OPG投与の臨床研究では，ビスホスホネートの1つであるパミドロネートと同等の骨吸収マーカー低下作用を有することが報告されている[9]。

最近やはりAmgen社のグループから，RANKLに対する完全ヒト型モノクローナル抗体（AMG162，denosumab）の開発が発表された。2005年の米国骨代謝学会では，denosumabによって中和されるchimeric RANKLをknock-inしたマウスを用いて，denosumabはFc-OPGに比べてもより強力な骨密度上昇作用を有することが報告された。Clinical trialにおいても，denosumabは一度の皮下投与によって閉経後骨粗鬆症の女性において数カ月という長期間にわたって骨代謝回転を低下させることが報告されている（図2）[10]。2005年の米国リウマチ学会では閉経後骨粗鬆症患者を対象にした第Ⅱ相試験において，半年に一度のdenosumab投与が骨密度増加作用を有することが報告された（表2）。

Fc-OPG，denosumabいずれも骨吸収抑制作用を有するという点でビスホスホネートと同じ骨吸収抑制剤に属すると考えられるが，興味深いことに，denosumabはアレンドロネートでは増加しない橈骨遠位部の骨密度を増加させること，カニクイザルを用いた研究で，皮質骨増加作用が強いことが報告されており，これまでの骨吸収抑制剤にない作用を有する可能性がある。

OPGあるいは抗RANKL抗体の問題点の1つとして，免疫系に対する作用があげられる。RANKLが活性化したT細胞に発現し，樹状細胞の生存を促進すること，RANKLやRANKノックアウトマウスでは末梢リンパ節の欠損を示すことなどから，RANKL-RANK

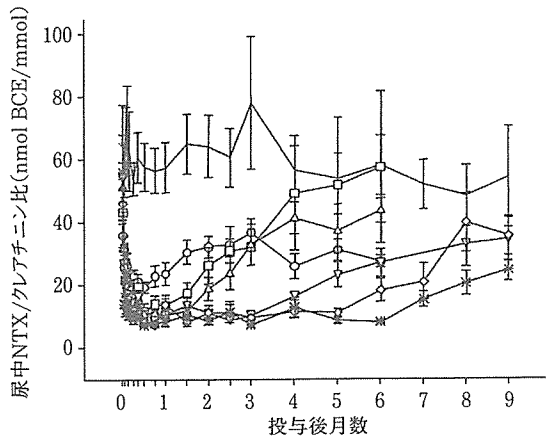

図2　閉経後骨粗鬆症患者における denosumab 投与の骨吸収マーカーに対する効果

印なし：プラセボ，○：0.01 mg/kg，□：0.03 mg/kg，△：0.1 mg/kg，▽：0.3 mg/kg，◇：1.0 mg/kg，＊：3.0 mg/kg

NTX：Ⅰ型コラーゲン架橋N-テロペプチド

denosumab 皮下注射によって持続的な NTX の低下が認められた。

（文献 10 より改変）

系の免疫機能に対する役割が示唆されている。これまでの臨床研究では Fc-OPG，抗 RANKL 抗体投与患者において免疫異常の報告はないが，今後も検討すべき課題であると考えられる。また，これらの治療薬がタンパク製剤であるため，中和抗体の産生とそれによる endogenous なタンパクの機能減弱が危惧される。実際に Fc-OPG 投与患者においては自己抗体の産生が報告されており，注意を要する点である。

ここでは骨粗鬆症の治療戦略として，抗 RANKL 抗体，あるいは OPG を用いた治療法の可能性を紹介した。現在日本ではこれらの薬剤は使用できず欧米でも臨床試験中の段階ではあるが，近年の骨粗鬆症の基礎・臨床研究の進展は目覚ましく，OPG，抗 RANKL 抗体など

表2　閉経後骨粗鬆症患者における denosumab による骨密度増加作用

	denosumab（すべての用量）[a]	denosumab 60 mg/6カ月[b]	アレンドロネート 70 mg/週[b]	プラセボ[b]
腰椎	4.25%～8.95%	7.37%±0.63%	6.22%±0.63%	−1.04%±0.68%
大腿骨近位部	2.76%～5.11%	5.11%±0.40%	3.40%±0.40%	−1.75%±0.43%
橈骨遠位1/3	0.59%～2.47%	1.77%±0.52%	−0.81%±0.55%	−2.82%±0.56%
全身	0.90%～4.46%	2.63%±0.50%	1.51%±0.52%	−1.62%±0.54%

[a]：すべての用量の平均値%変化，[b]：骨密度変化の平均値±標準誤差

（2005 年米国リウマチ学会抄録 L25 より改変）

を用いた骨粗鬆症治療が実際に臨床応用される日も遠くないと考えられる。

（田中　栄）

■文　献

1) Mashiba T, Turner CH, Hirano T, et al：Effects of high-dose etidronate treatment on microdamage accumulation and biomechanical properties in beagle bone before occurrence of spontaneous fractures. Bone 29：271-278, 2001
2) Odvina CV, Zerwekh JE, Rao DS, et al：Severely suppressed bone turnover：a potential complication of alendronate therapy. J Clin Endocrinol Metab 90：1294-1301, 2005
3) Whyte MP, Wenkert D, Clements KL, et al：Bisphosphonate-induced osteopetrosis. N Engl J Med 349：457-463, 2003
4) Ruggiero SL, Mehrotra B, Rosenberg TJ, et al：Osteonecrosis of the jaws associated with the use of bisphosphonates：a review of 63 cases. J Oral Maxillofac Surg 62：527-534, 2004
5) Theill LE, Boyle WJ, Penninger JM：RANK-L and RANK：T cells, bone loss, and mammalian evolution. Annu Rev Immunol 20：795-823, 2002
6) Rodan GA, Martin TJ：Role of osteoblasts in hormonal control of bone resorption — a hypothesis. Calcif Tissue Int 33：349-351, 1981
7) Eghbali-Fatourechi G, Khosla S, Sanyal A, et al：Role of RANK ligand in mediating increased bone resorption in early postmenopausal women. J Clin Invest 111：1221-1230, 2003
8) Bekker PJ, Holloway D, Nakanishi A, et al：The effect of a single dose of osteoprotegerin in postmenopausal women. J Bone Miner Res 16：348-360, 2001
9) Body JJ, Greipp P, Coleman RE, et al：A phase I study of AMGN-0007, a recombinant osteoprotegerin construct, in patients with multiple myeloma or breast carcinoma related bone metastases. Cancer 97：887-892, 2003
10) Bekker PJ, Holloway DL, Rasmussen AS, et al：A single-dose placebo-controlled study of AMG 162, a fully human monoclonal antibody to RANKL, in postmenopausal women. J Bone Miner Res 19：1059-1066, 2004

4．新しい治療薬
④ 新しいSERM

エストロゲンは骨，乳房，子宮などの組織で多様な効果を発揮している。したがって，閉経後にはエストロゲン欠失による多彩な身体的変化が引き起こされる。そこでエストロゲン作用の利点を抽出し，必要な効果のみを再現する化合物の開発が精力的に行われてきた。そのような効果を発揮できる一群の化合物に，選択的エストロゲン受容体調整剤（SERM：selective estrogen receptor modulator）があり，臓器特異的にエストロゲン様の作用を示したり，抗エストロゲン作用を発揮する。SERMはエストロゲンとは異なりステロイド骨格をもたず，基本骨格から図1のように分類されている[1]。また，時に植物性エストロゲンを含む表記もなされる。現在，臨床に供されているSERMには骨粗鬆症治療薬のラロキシフェンと乳がんに適応をもつタモキシフェンがあり，さらにいくつかの化合物が開発治験の途上にある。

SERMの作用メカニズム

SERMが組織特異性や化合物間の差異を示すのは，リガンド・受容体複合体の構造変化に由来すると現在では説明されている[2]。エストロゲンとは違いステロイド骨格をもたないことで，リガンド・受容体複合体の立体構造はエストロゲン自体が関与する場合と異なり，それぞれの組織において作用発現に必要な転写共役因子（促進因子：co-activator，抑制因子：co-repressor）との結合性が変化し，その変異と転写共役因子との相互作用が，組織選択的な薬理効果発現につながると考えられている。たとえば子宮内膜がんに対しては，第1世代のSERMであるタモキシフェンがその危険率を増すのに対して，新世代SERMのラロキシフェンは危険性に影響を及ぼさないことが知られている[3]。また，SERMの組織選択的な薬理効果にエストロゲン受容体α型およびβ型を介した，特異な効果がある

II-1　カルシウム調節ホルモンとしての活性型ビタミンD

2）骨および標的臓器に対する作用

ビタミンDの代謝

くる病という小児の骨疾患の存在，そしてこの疾患と日光照射との関係は古くから知られていた[1]。ビタミンDは抗くる病因子として発見された脂溶性ビタミンであるが，脊椎動物では皮膚のケラチノサイト膜表面に大量に存在するプロビタミンD(7-デヒドロコレステロール)が紫外線(波長290～315 nmの中波長紫外線)照射によって9位と10位との間に非酵素的な開裂反応が生じて不安定なプレビタミンDとなり，これが熱で異性化されてビタミンDとなる[2]。植物から得られるビタミンDはビタミンD_2であるが，動物の体内で合成されるものはすべてビタミンD_3系である。体内で合成された，あるいは食物から摂取されたビタミンD_3は肝臓で25位が，腎臓で1α位が水酸化されることによって活性型である1α,25-ジヒドロキシビタミンD_3 ($1\alpha,25(OH)_2D_3$)となる。肝細胞における25位の水酸化にはミトコンドリア内膜に存在するCYP27A1が関与すると考えられているが，*CYP27*遺伝子のノックアウトマウスではビタミンD代謝に異常は認められず，少なくとも25位水酸化の主たる担い手ではないようである[3]。CYP27A1以外にはミクロソーム画分に存在するCYP2D25あるいはチトクロームP450 CYP2R1が25水酸化酵素の候補として挙げられている。特に*CYP2R1*遺伝子の不活性型変異によって$25(OH)D_3$欠損を来した症例が報告されており，ビタミンDの25位水酸化におけるCYP2R1の重要性が注目されている[4]。今後ノックアウトマウスなどによる証明が待たれる。

$25(OH)D_3$はα_2グロブリン画分に存在するビタミンD結合蛋白(vitamin D-binding protein: DBP)に結合して血中を運搬される。腎臓ではDBPに結合した$25(OH)D_3$が近位尿細管に存在するリポ蛋白様受容体であるメガリンに結合して細胞内に取り込まれ，ミトコンドリア内でCYP27B1によって1α位が水酸化され，活性型の$1\alpha,25(OH)_2D_3$が産生される。メガリン欠損マウス，あるいは腎特異的なメガリンノックアウトマウスではビタミンD欠乏性くる病様の病態を示すことからも，ビタミンD代謝におけるメガリンの重要性が確認されている[5,6]。メガリンを介した取込みができない腎以外の組織では，DBPに結合していないビタミンD代謝産物のみが細胞内に取り込まれる。CYP27B1の発現レベルは腎近位尿細管で最も高いが，ヒトケラチノサイトやマウスマクロファージにおいても高い発現レベルを認める。

1α水酸化酵素活性は$1\alpha,25(OH)_2D_3$や副甲状腺ホルモン(PTH)をはじめとするさまざまなホルモン，サイトカインによって厳密に調節されており，ビタミンD受容体(vitamin D receptor: VDR)ノックアウトマウスでは高い活性を示す。最近では老化遺伝子として発見されたKlothoが1α水酸化酵素活性を負に調節することが明らかになっている[7]。ビタミンD依存性くる病I型患者ではヒト*CYP27B1*遺伝子に変異があるために腎における$1\alpha,25(OH)_2D_3$産生に異常を示すこと，*CYP27B1*ノックアウトマウスではくる病になることから，CYP27B1がビタミンDの1α水酸化において決定的な役割を果たすことが明らか

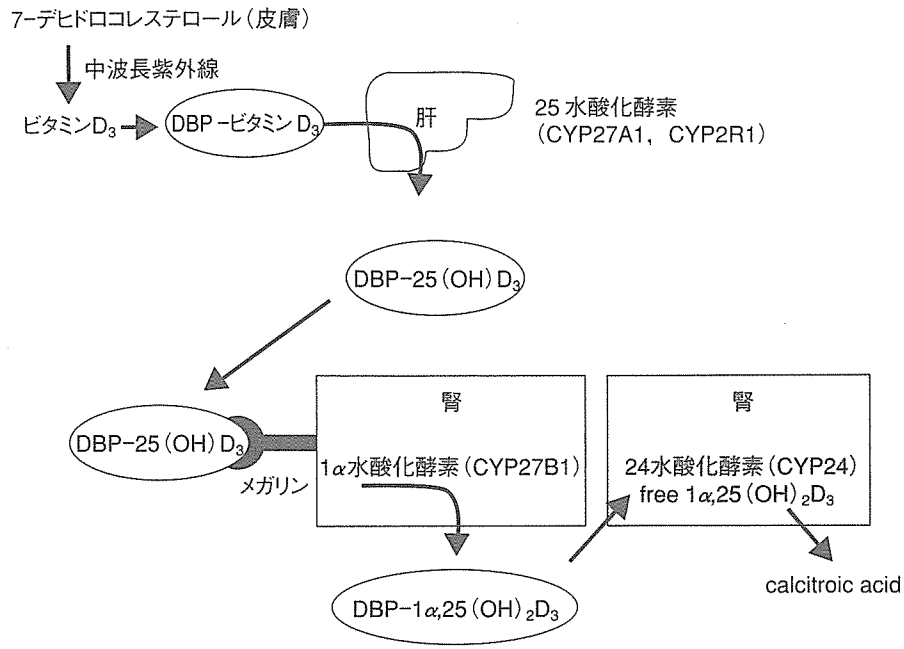

図 1　ビタミン D_3 の代謝経路とその代謝産物
（文献 1 より改変）

になっている[8,9]。興味深いことに，CYP27B1 欠損マウスにおけるくる病は 1α,25(OH)$_2D_3$ 投与によってレスキューされるが，高カルシウム・高リン・高ラクトース食（レスキュー食）では骨の異常が完全には回復しないことが報告されている。

一方で，腎臓には 24 水酸化酵素である CYP24 が存在し，24 位の水酸化を担うことによってビタミン D のカタボリズムに重要な役割を果たす。CYP24 の発現は 1α,25(OH)$_2D_3$ によって厳密に調節されており，CYP24 ノックアウトマウスは 1α,25(OH)$_2D_3$ 投与によって容易にビタミン D 過剰による腎障害を呈する[10]。**図 1** はビタミン D_3 の代謝経路をまとめたものである。

1α,25(OH)$_2D_3$ は特異的な核内受容体である VDR に結合して機能を発揮する。この結合によって VDR はダイナミックな三次元構造の変化を来し，9-シスレチノイン酸を結合するレチノイド X 受容体（RXR）とヘテロ二量体を形成して，遺伝子のプロモーター配列に存在するビタミン D 応答配列（VDRE）に結合することによって，さまざまな 1α,25(OH)$_2D_3$ 依存性の遺伝子発現を誘導する。VDR ホモ欠損マウスにおいては離乳までは正常に成長するが，離乳後（3 週齢）より成長障害が明らかになり，生後 5 週目から著明なくる病症状を示す[11,12]。ホモ欠損マウスのくる病は高カルシウム，高リン食によってレスキューされるが，もう一つの特徴である全身の脱毛現象は回復しない。この結果は皮膚がビタミン D の重要な直接標的臓器であることを示している。

VDR を介する機能発現（genomic action と呼ばれる）以外に，膜に存在する受容体を介した作用機序，いわゆる non-genomic action が存在することが以前から報告されているが，その生理的作用は未だに明らかではない。

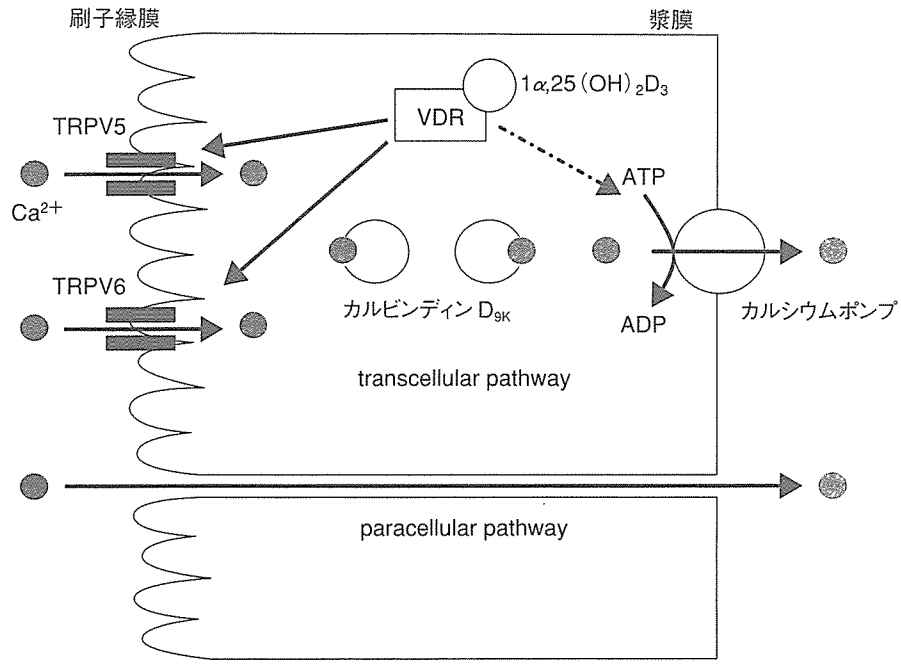

図 2　小腸におけるカルシウム吸収のメカニズムとビタミン D の作用
（文献 1 より改変）

活性型ビタミン D の標的臓器

1）小腸

腸管からのカルシウム吸収能は高い順に回腸＞空腸＞十二指腸となっているが，VDR 発現は十二指腸で最も多く，$1\alpha,25(OH)_2D_3$ はカルシウム吸収能を促進する。カルシウム吸収機序としては paracellular pathway，transcellular pathway が存在することが知られている。paracellular pathway においてはカルシウムが上皮細胞の tight junction を通って吸収され，transcellular pathway では上皮細胞内を通過して吸収される。transcellular pathway においては小腸の apical side（刷子縁側）に存在するカルシウムチャネル（CaT1 あるいは TRPV6）および上皮のカルシウムチャネル（ECaC1 あるいは TRPV5）によるカルシウムの取込み[13,14]，カルビンディンによる細胞内輸送[15]，そして漿膜側からのカルシウムポンプ（Ca-ATPase, PMCA1b）による排出を介して行われる[16]（図 2）。近年，カルシウム吸収におけるビタミン D の機能が VDR ノックアウトマウスにおいて詳細に解析された。異なる施設で作製されたノックアウトマウスにおいてその表現型は多少異なるが，すべてに共通する表現型として十二指腸における CaT1，ECaC1 レベルの低下が認められた[11]。一方ノックアウトマウスと正常マウス間で Ca-ATPase の発現に差は認められなかった。以上の結果は，ビタミン D が主としてカルシウム流入の調節を介してカルシウム吸収を制御していることを示している。

2）腎

先にも述べたように，腎臓は $1\alpha,25(OH)_2D_3$ 産生およびカルシウムの再吸収において中心的な役割を果たす。VDR 欠損マウスにおいては腎遠位尿細管におけるカルシウム再吸収に障害があり，そのために尿中のカルシウム排泄が亢進し，低カルシウム血症になること